

A Microarray Study to Characterize the Molecular Mechanism of TIMP-3-Mediated Tumor Rejection

Paula Lam, Kar Sian Lim, Suk Mei Wang, and Kam M. Hui*

Gene Vector Laboratory, Division of Cellular and Molecular Research, National Cancer Centre, 11 Hospital Drive, Singapore 169610

*To whom correspondence and reprint requests should be addressed. Fax: (65) 6226 3843. E-mail: cmrhkm@nccs.com.sg.

Available online 25 April 2005

Glial cell invasion is a multistep cellular process that involves a complex system of tightly regulated proteases (matrix metalloproteinases; MMPs) and their endogenous inhibitors (tissue inhibitors of metalloproteinases; TIMPs) to mediate the degradation of the basement membrane and extracellular matrix. Tissue inhibitor of metalloproteinases-3 (TIMP-3) is a matrix-bound inhibitor of MMPs. In the present study, we have overexpressed the *TIMP3* gene in human glioma cells with a herpes simplex virus type 1 amplicon-based vector. Oligonucleotide DNA arrays were employed to identify genes that were differentially modulated by the overexpression of TIMP-3. Consistent with the function of TIMP-3, genes associated with angiogenesis, growth factors, cytokines, death receptors, and substrates of the various MMPs were found to be up-regulated. Furthermore, caspases are important in the signaling pathway of cellular apoptosis, and the overexpression of TIMP-3 in glioma cells is tightly associated with the activation of caspases, including caspase-1, at both the mRNA level ($P = 0.0371$) and the protein level. Moreover, the activation of an apoptotic pathway via the overexpression of TIMP-3 induced apoptosis of transduced human glioma cells *in vitro* and the growth inhibition of human glioma tumor xenografts in immunodeficient mice.

Key Words: HSV-1 amplicon viral vectors, TIMP-3, glioma, apoptosis, caspase cascade, microarray

INTRODUCTION

Glioblastoma multiforme (WHO grade IV) is the most frequent malignant brain tumor to affect adults. Glioblastomas do not metastasize and rarely disseminate through cerebrospinal fluid. However, they do invade the surrounding normal brain, which is a multistep process that is dependent on the ability to degrade basement membranes and extracellular matrix (ECM) in an effective and controlled manner [1]. The turnover of ECM components is subsequently controlled by a complex system of tightly regulated protease enzymes, including the serine proteases, the metalloproteinases (MMPs), and the plasminogen activation system. Although human gliomas express other proteases, MMPs seem to be responsible for much of the degradation of a broad range of ECM components contributing to tumor cell invasion [2,1].

Metalloproteinases are a family of at least 20 zinc-dependent endopeptidases collectively capable of degrading essentially all ECM components, including collagens, fibronectin, laminin, and basement membrane proteoglycans [3,4]. MMPs have been grouped according to their substrate specificities, i.e., collagenases, gelatinases,

stromelysins, and the membrane-type MMPs. The membrane-type MMPs comprise six members of plasma membrane-tethered MMPs, which include four type I transmembrane enzymes, MT1-, MT2-, MT3-, and MT5-MMP (known as MMP-14, -15, -16, and -24, correspondingly), and two glycosylphosphatidylinositol-anchored enzymes (MT4-MMP/MMP-17 and MT6-MMP/MMP-25) [5]. Elevated levels of MMP-2, MMP-9, and MT1-MMP have been found in gliomas compared to normal brain tissues [6].

A major mechanism for controlling MT-MMP activity in the pericellular space is mediated by the action of tissue inhibitors of metalloproteinases (TIMPs), which bind to active MMPs in a 1:1 molar stoichiometry [7]. An imbalance between MMP and TIMP activity leading to excess degradation of the ECM has been shown to be associated with a certain number of pathologic conditions, including tumor growth and metastases [8]. Thus, inhibitors of MMPs could potentially be useful for blocking cancer progression. There are four family members (TIMP-1, TIMP-2, TIMP-3, and TIMP-4) that share similar genomic organization, tertiary structure, and ability to inhibit MMP activity [9,10]. Essentially, each of the four

TIMPs can nonselectively bind to all MMPs, with one exception being the inability of TIMP-1 to inhibit effectively members of MT-MMPs as described earlier [11]. Furthermore, only TIMP-3 is a good inhibitor of tumor necrosis factor- α -converting enzyme (TACE/ADAM-17), which belongs to another group of metalloproteinases [12].

Generally, TIMP-1, TIMP-2, and TIMP-4 have been reported to exert antiapoptotic effects [13–15]. Unlike other TIMPs, TIMP-3 localizes to the ECM and can affect cell growth and survival [8]. Previous data have shown that TIMP-3 protein can induce apoptosis in certain cell lines, while its overexpression has no effect on other cell types [16]. Recently, it has been suggested that TIMP-3 could inhibit shedding of death receptors from the cell surface [17–19] and as a consequence, lead to the activation of an apoptotic signaling pathway. Other reports also suggest that TIMP-3 activates the mitochondrial apoptotic pathway in a FADD-dependent manner [20]. The exact mechanism of the effects of TIMP-3 has not yet been fully elucidated and could be resolved only when the relevant MMPs or ADAM substrates are identified. Furthermore, the majority of studies reporting on the overexpression of TIMP-3 were mediated by recombinant adenoviral vector. However, it is possible that adenoviral vectors could, on their own, elicit strong host immune responses to result in cell death; it would therefore be of interest to determine if an alternative viral vector system that is relatively nonimmunogenic could mediate the stable expression of TIMP-3 to activate the apoptosis pathway and provide on-site protection to recurrent glioma tumors. In the present study, genes that are differentially expressed following herpes simplex virus type 1 (HSV-1) amplicon-mediated overexpression of TIMP-3 in human gliomas are identified using oligonucleotide microarray-based analyses to gain insights into the effects of TIMP-3 on the survival of the transduced cells.

RESULTS AND DISCUSSION

Identification of Genes That Are Differentially Expressed in Human Glioma Cells with Elevated Timp-3 Expression Mediated by HSV-1 Amplicon Vector

We used the reverse transcription-polymerase chain reaction (RT-PCR) to facilitate the cloning of the wild-type human TIMP-3 cDNA (~650 bp) into the HSV-1 amplicon plasmid pHGCX to generate HSV-sTIMP-3. The parental backbone vector amplicon plasmid, pHGCX, is a pBR322-based plasmid containing HSV-1 *ori_s* and *pac* signals. The gene encoding the enhanced green fluorescence protein (eGFP), under the control of the HSV-1 immediate early promoter (IE 4/5), allows the titration of viruses [22]. The gene of interest, i.e., *TIMP3* is driven by the CMV IE promoter and this construct is designated as

HSV-sTIMP-3. As a control to ensure that the transgene activity observed was not due to the viral backbone, we also inserted the TIMP-3 cDNA in the opposite orientation and this antisense TIMP-3 construct is designated as HSV-aTIMP-3. We verified all inserted DNA fragments by DNA sequencing reactions (Applied Biosystems, Inc., USA). These amplicon plasmids were subsequently packaged into infectious HSV-1 amplicon virions, using the helper virus-free packaging system [23]. Viral titers of the helper virus-free backbone vector, HSV-sTIMP-3, and HSV-aTIMP-3 ranged from 1×10^6 to 1×10^7 transduction units per milliliter (TU/ml) following concentration by sucrose gradient centrifugation.

The endogenous level of TIMP-3 protein in Gli36 cells was only barely detectable by Western blot analysis (Fig. 1A). To determine whether the HSV-sTIMP-3 viral construct could mediate the stable expression of the TIMP-3 protein, we infected human glioma Gli36 cells with HSV-sTIMP-3 viruses at a multiplicity of infection (m.o.i.) of 1.0. We observed a high level of TIMP-3 protein by Western blot analysis (Fig. 1A). The molecular weight (MW) of the TIMP-3 was approximately 24 kDa and represents the unglycosylated forms of TIMP-3. In addition, the MW of the TIMP-3 protein detected was also similar to that of the commercially available TIMP-3 protein (Chemicon, Temecula, CA, USA) and acted as the positive control in our present study. No TIMP-3 could be detected in the conditioned medium of HSV-aTIMP-3-infected Gli36 cells at the various time points assayed within 72 h (data not shown).

In an attempt to identify genes that are modulated by the overexpression of TIMP-3 in human glioma cells, we performed high-density oligonucleotide microarray analyses using total RNA extracted from HSV-sTIMP-3-infected Gli36 cells at 72 h postinfection (p.i.). We employed the Affymetrix GeneChip Human Genome HG-U133A oligoarray that features approximately 14,500 genes (over 22,000 transcripts) from the Human UniGene database (build 133A) in our study. We selected differential changes in gene expression profiles related to elevated TIMP-3 expression by comparison of gene expression profiles between RNA samples of uninfected cells and those of TIMP-3-infected Gli36 cells. We filtered the raw data obtained from the Affymetrix gene chips at a signal-log ratio (SLR) of 0.26 (≥ 1.2 -fold) for up-regulated genes and similarly, we used an SLR of -0.26 (≤ 1.2 -fold) to filter out the down-regulated genes. We observed that a total of 707 genes were differentially down-regulated and 2283 genes were differentially up-regulated 72 h following infection with HSV-sTIMP-3.

It has been suggested that TIMP-3 could activate certain signaling pathways that control cell death. We were therefore interested in identifying those genes that were modulated by the elevated level of TIMP-3 and known to play a role in cellular processes related to apoptosis. In our study, there were 45 apoptosis-related

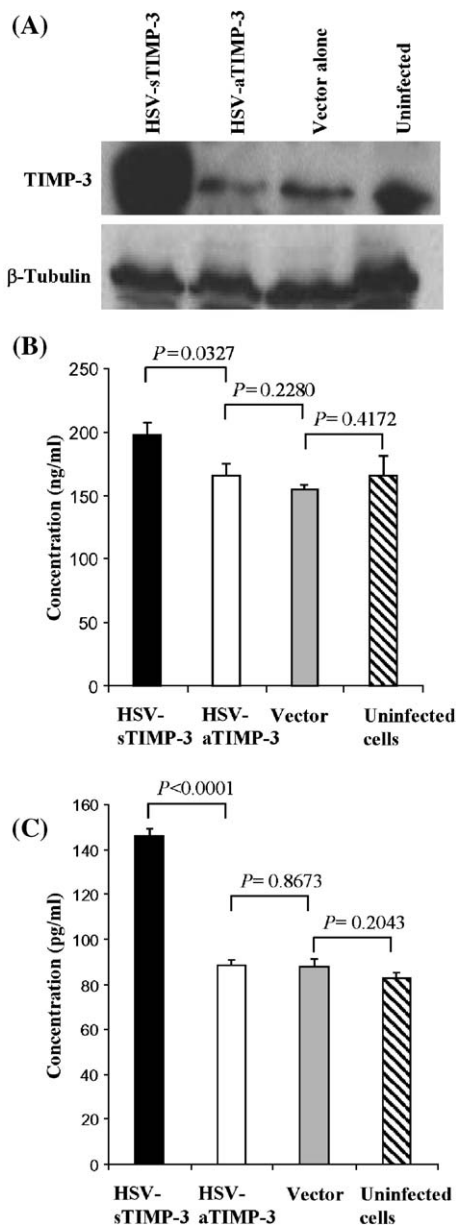


FIG. 1. TIMP-3-induced elevated expression of TNF- α proteins and caspase-1 protein. (A) Western blot detecting TIMP-3 overexpression in the extracellular matrix of viral vector-infected (m.o.i. 1.0, 72 h p.i.) and uninfected Gli36 cells. β -Tubulin was used as a control for equal protein loading. (B) ELISA showed elevated expression of TNF- α protein (\sim 1.2-fold) in HSV-sTIMP-3-transduced Gli36 cells compared with controls consisting of uninfected cells, vector alone, or cells infected with HSV-aTIMP-3 ($P < 0.05$). (C) Caspase-1 protein level was \sim 1.8-fold higher in HSV-sTIMP-3-transduced Gli36 cells compared with uninfected cells and \sim 1.7-fold higher compared with cells infected with either the HSV-aTIMP-3 or the backbone vector ($P < 0.05$). All ELISAs were performed at 72 h p.i. (m.o.i. 1). Data shown represent averages from experiments performed in triplicate \pm SEM.

genes. Notably, elevated levels of many metalloproteinase transcripts, including ADAM-9, ADAM-10, ADAM-17, ADAM-19, ADAM-21, and ADAM-23, were detected at

72 h p.i. (see supplementary information). TIMP-3 is known to inhibit the activities of membrane-anchored proteinases, including ADAMs such as TACE/ADAM-17 [12], ADAM-10 [26], ADAM-12 [27], and ADAM with thrombospondin-like repeats aggrecanase-1 (ADAM-TS4) and aggrecanase-2 (ADAM-TS5) [28]. One possible explanation for the observed high level of ADAM members may be the inhibition of the metalloproteinase-dependent shedding of death receptors by TIMP-3. The ADAM protease family could act as ectodomain sheddases in the removal of cell surface death receptors and death-inducing ligands. Thus, in the absence of TIMP-3, metalloproteinase-dependent shedding of death receptors from the cell surface results in suppression of death receptor signaling and promotes cell survival [19]. When TIMP-3 is present, death receptor shedding is prevented, leading to a subsequent accumulation of metalloproteinases. Ligands binding to death receptors that were not shed enable the activation of the apoptotic pathway. Interestingly, the expression of only a small number of genes was down-regulate and this included the ADAM-TS1 gene (also known as METH-1) (see supplementary information). The function of ADAM-TS1 is still poorly understood. Unlike many of the ADAM proteases, ADAM-TS1 does not have a transmembrane domain and is consequently preferentially secreted into the ECM, where it binds via the thrombospondin motifs [29].

In particular, ADAM-17 has been implicated in the shedding of numerous cell surface proteins, including TNF- α [30], transforming growth factor- α (TGF- α), and L-selectin [31]. Although ADAM-17 was up-regulate following transduction of Gli36 cells with HSV-sTIMP-3, TNF- α was not up-regulated when analyzed with microarrays. Nevertheless, it was interesting to note that the level of TNF- α in HSV-sTIMP-3-transduced Gli36 cells was comparatively higher than the controls when studied with enzyme-linked immunosorbent assay (ELISA) (Fig. 1B). Furthermore, we observed that the TNF- α -inducible proteins 1, 2, 3, and 8 are all up-regulated, with fold changes ranged from 1.26 to 1.57, following transduction of Gli36 cells with HSV-sTIMP-3, although only TNF- α -inducible protein 1 (TNFAIP1) is statistically significant (see supplementary information).

Cell Death Induced by TIMP-3 is Mediated via the Caspase Cascade

Following transduction of Gli36 cells with HSV-sTIMP-3, the detectable level of TIMP-3 was 2.7-fold above that of the control cells ($P = 0.032$). Recent studies have identified epidermal growth factor-containing fibulin-like extracellular matrix protein 1 (EFEMP1; also known as fibulin 3) as a protein that interacts strongly with TIMP-3 in the subretina region [32]. EFEMP1 belongs to the fibulin family, which is a newly emerging family of six secreted glycoproteins. Interestingly, in addition to EFEMP1, we found EFEMP2 to be up-regulated in HSV-

stIMP-3-infected Gli36 cells. Both fibulins 1 and 2 were significantly elevated on repeated experiments (P values = 0.01541 and 0.02904, respectively) and have been hypothesized to be important in the assembly and stabilization of ECM structures and may regulate organogenesis, vasculogenesis, fibrogenesis, and tumorigenesis [33]. These findings open the possibility that EFEMP1 and 2 could be potential targets of interaction with TIMP-3. TIMP-3 has been indicated to be an effective inhibitor of a number of substrates, including cellular components that belong to the ECM, growth factors/cytokines, and factors involved in angiogenesis and apoptosis. To dissect further the molecular pathways through which TIMP-3 triggers apoptosis, we have focused on the genes that could be classified into these four categories (see supplementary information).

The total number of genes that could be associated with apoptosis and whose expression was modulated 72 h following transduction of Gli36 cells with HSV-stIMP-3 is estimated to be approximately 13% of all the available apoptosis-related genes on the HG-U133A gene chip. Among the up-regulated genes are three members of the TNF receptor family, namely the tumor necrosis factor receptor superfamily member 5 (TNFRSF5 or CD40), TNFRSF6 (also known as CD95/FAS), and TNFRSF6B (or decoy receptor 3); death receptor 6 (TNFRSF21); and the tumor necrosis factor (ligand) superfamily member 9 (TNFSF9). Ahonen *et al.* recently showed that adenoviral-mediated TIMP-3 expression resulted in the stabilization of the three death receptors TNF-RI (or TNFRSF1A), FAS (TNFRSF6), and TRAIL-RI (or TNFRSF10A) on the cell surface, which thus enabled the transduced human melanoma cells to be more susceptible to apoptosis induced by specific ligands [19]. Our results showed that overexpressed TIMP-3 induced an elevated level of FAS transcripts that was 1.5-fold higher compared to controls ($P = 0.0376$). TNFRSF10A was not studied since it was not present on the HG-133A probe array. In addition, we found TNFRSF5, TNFRSF6B, and TNFRSF21 also to be up-regulated. Therefore, our results tend to suggest that TIMP-3-induced apoptosis in human glioma cells could be mediated through different tumor necrosis factor receptors. Other detectable and well-characterized death receptors and domains are listed in Table 1.

Among 22 MMPs that are present on the HG-133A probe array, MMP2/gelatinase A ($P = 0.0244$) and MMP9/gelatinase B ($P = 0.037$) were the only detectable transcripts that were elevated at 72 h p.i. compared to control cells (see supplementary information). In addition, substrates of MMP2 and MMP9 such as collagen types IV and V were also found to be elevated. Similarly, other matrix substrates including CD44, laminin, and fibronectin were also up-regulated.

Apart from their direct roles in ECM degradation and cell invasion, MMPs could also cleave growth factors and their receptors, cytokines, and cell-cell and cell-matrix

TABLE 1		
	72 h p.i (Fold change)	t-test
<i>BCL-2 family</i>		
BCL2L13	1.223	0.04933
BNIP1	1.551	0.004808
BNIP3	1.681	0.03569
BNIP3L	1.866	0.004683
MOAP1	1.355	5.14E-05
<i>CASPASE family</i>		
CASP1	4.943	0.03705
CASP4	1.751	0.04116
CASP7	1.203	0.04043
CASP8	1.878	0.01167
CASP8AP2	1.403	0.02365
<i>IAP family</i>		
BIRC5	1.243	0.03685
<i>TRAF family</i>		
TANK	1.527	0.01126
<i>CARD family</i>		
BCL10	2.009	0.01016
RIPK2	1.228	0.04234
<i>Death Domain family</i>		
ANK2	1.243	0.0417
CRADD	1.288	0.0336
NFKB2	1.368	0.0403
TRADD	1.457	0.0456
<i>Death Effector Domain family</i>		
CFLAR	1.408	0.00812
FADD	1.311	0.03905
<i>CIDE Domain family</i>		
DFFA	1.316	0.0498
<i>p53 pathway</i>		
GADD45A	2.113	0.0426
PERP	1.225	0.0431
<i>TNF Receptor family:</i>		
TNFRSF5	1.331	0.0022
TNFRSF6	1.457	0.0376
TNFRSF6B	1.389	0.0451
TNFRSF21	2.756	0.04893
<i>TNF ligand family:</i>		
TNFSF9	1.297	0.0238
<i>Others</i>		
DATF1	2.204	0.047
DPF2	1.386	0.02862
PDCD4	1.421	0.03849
PDCD6	1.257	0.01409

adhesion molecules [34]. Many of these molecules were up-regulated in our study at 72 h p.i. These are the epidermal growth factor receptor and one of its ligands,

TGF- α ; platelet-derived growth factors; fibroblast growth factor and its receptors; transforming growth factors; erythropoietin receptor; insulin-like growth factor receptors; interleukin-1A, interleukin 1B; and tumor necrosis factor and its receptors. Above all, vascular endothelial growth factors B and C (VEGFB and VEGFC), VEGF (also known as VEGFA or VEGA), and neuropilin-1 (NRP1 or NPN1) were also up-regulated (see supplementary information). Interestingly, TIMP-3 has recently been reported to inhibit downstream signaling and angiogenesis pathways by blocking the binding of VEGF to VEGF receptor-2 [35]. The relatively high level of VEGF detected in our study could therefore be a consequence of the failure of VEGF to bind to its receptors, resulting from elevated TIMP-3 expression in the human glioma cells. This observation is consistent with data reported by Sallinen *et al.*, who showed that glioblastomas are highly vascular tumors that often overexpress vascular endothelial growth factor in comparison to normal brain [36].

By 72 h p.i., proapoptotic genes belonging to the Bcl-2 family such as BNIP3 and BNIP3L were all up-regulated (Table 1). All five contiguous probe sets representing caspase-1 were up-regulated and its overall expression was 5-fold higher than that of the control group ($P = 0.037$). Caspase-3 and caspase-7 were each represented by only one probe set on the HG-U133A gene chip. At 72 h p.i., the level of caspase-3 in Gli36 cells following transduction with HSV-sTIMP-3 remained unchanged, while the levels of caspase-4 and caspase-7 in Gli36 cells following transduction with HSV-sTIMP-3 were up-regulated by 1.75- and 1.2-fold, respectively (Table 1). The activated "initiator" caspase-8 (also known as FLICE) instigates the activation of intracellular "executioner" caspases, including caspase-1, -3, and -7. Our results therefore suggest that TIMP-3 may be most likely to induce the caspase-dependent apoptotic death pathways in glioma cells. To find out if overexpression of TIMP-3 induces predominantly genes involved in the apoptotic pathways, we analyzed all up-regulated genes further using the GoSTAT gene ontology mining tool (<http://gostat.wehi.edu.au>) [37]. This approach revealed that up-regulation of genes related to programmed cell-death pathways is statistically significant (P value 3.2×10^{-8}) using the Benjamini and Hochberg correction controls. Furthermore, we performed ELISA and found the level of caspase-1 expression in HSV-sTIMP-3-transduced Gli36 cells to be 5-fold higher than that of the control groups of cells (Fig. 1C, $P < 0.0001$). However, it is unclear to us whether the two principle pathways consisting of death receptors and members of the Bcl-2 family were induced by TIMP-3 independently or whether they influence each other, resulting in the regulation of apoptosis. Nevertheless, both pathways have the same outcome, which is the activation of a cascade of proteolytic enzymes, members of the caspase family. Two categories of caspases that are important for apoptosis have been

recognized. These are the initiators and executioner caspases [38]. The initiator caspases, such as caspase-8 and -9, are activated during the earlier phase of apoptosis, while the executioner caspases, such as caspase-1, are activated as cells enter the later stages of the apoptotic pathway. Furthermore, we also noticed the activation of DNA damage and repair genes such as GADD45A (2.1-fold, $P = 0.0426$) following the elevation of TIMP-3. It is therefore also possible that the apoptosis of human glioma cells observed in our study could be partially a result of DNA damage.

The Apoptotic Effect of TIMP-3 in Glioma Cells

The percentages of transduction efficiencies in Gli36 cells were approximately 55 and 68% with the backbone viral vector and the HSV-aTIMP-3 construct, respectively, when estimated by analyzing for green fluorescent cells via FACS analysis (data not shown). The observed percentage of transduction efficiency for HSV-sTIMP-3 in Gli36 cells was 35%, which was relatively lower than that obtained with the backbone viral vector and the HSV-aTIMP-3 construct. This could possibly be due to the large number of cells that were transduced but were dead and were subsequently removed during the cell harvesting process for FACS.

We also studied the mechanism of apoptosis in Gli36 glioma cells following transduction with HSV-sTIMP-3 using cell viability and terminal deoxynucleotidyltransferase-mediated nick end labeling (TUNEL) staining. At various time points, we counted viable adherent cells from triplicate cultures using trypan blue exclusion assay. Our results showed that HSV-sTIMP-3-transduced Gli36 cells experienced a significant decrease in cell viability with time. The decrease in cell viability was not observed with cells that were infected with HSV-aTIMP-3 (Fig. 2A). We observed similar apoptotic effect results with other human glioma cells, including U251 and SF767, infected with HSV-sTIMP-3 (data not shown). In addition, we observed that HSV-sTIMP-3 could specifically induce cytoplasmic shrinkage and cell lysis of the transduced glioma cells that were not detectable in cells transduced with the HSV-aTIMP-3 construct (Fig. 2B). We further performed TUNEL-based assays with the detection of DNA strand breaks associated with apoptosis using enzymatically labeled digoxigenin nucleotides, which were allowed to bind to anti-digoxigenin antibody that was conjugated to a rhodamine reporter molecule. Confocal microscopy studies demonstrated colocalization of eGFP and DNA strand breaks associated with apoptosis in Gli36 cells transduced with HSV-sTIMP-3, indicated by the presence of the green color of eGFP and red coloration associated with rhodamine (Fig. 2C). The percentage of cells that were positively transduced with the HSV-sTIMP-3 amplicon viral vectors and were also undergoing apoptosis was 26%. In comparison, normal and proliferative nuclei that contained relatively insignificant

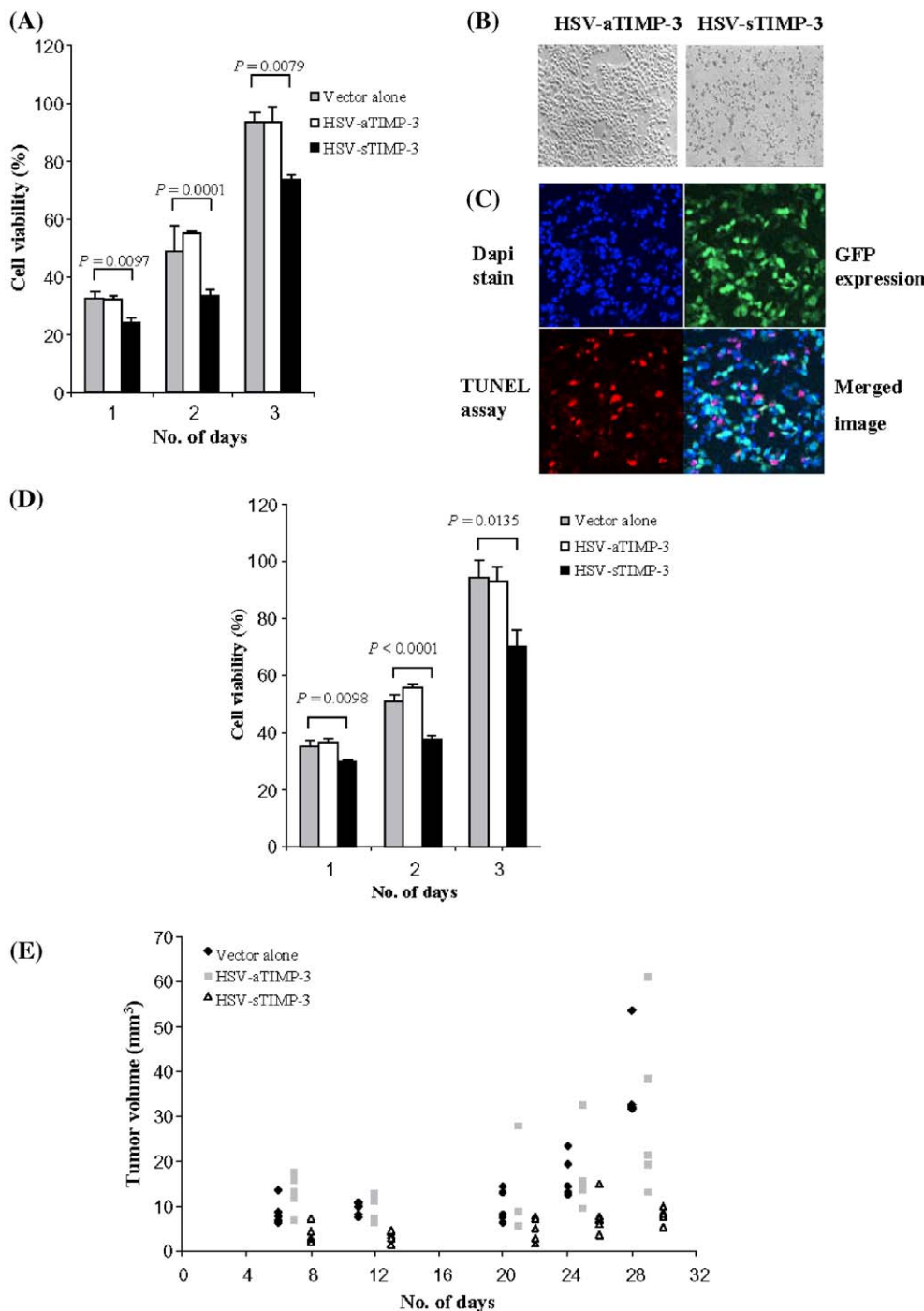


FIG. 2. *In vitro* inhibition and suppression of human glioma xenografts mediated by HSV-sTIMP-3 amplicon viral vectors. (A) Human glioma (Gli36) cells were infected with backbone, HSV-aTIMP-3, or HSV-sTIMP-3 amplicon viral vector at m.o.i. of 1. At various time points postinfection, adherent cells were counted using the trypan blue exclusion assay. Data shown represent averages from experiments performed in triplicate \pm SEM. (B) Cellular morphology of Gli36 cells infected with HSV-aTIMP3 and HSV-sTIMP-3. (C) Infected Gli36 cells (m.o.i. 1; 72 h p.i.) expressed the enhanced green fluorescence protein and cells undergoing apoptosis appeared red in color in TUNEL assay. (D) Cytotoxicity assay of U87MG cells infected using conditions similar to those described for (A). Data shown represent averages from experiments performed in triplicate \pm SEM. (E) Flanks of SCID mice inoculated with U87MG tumor cells were injected with the three different amplicon viruses as mentioned in (A). The tumor volume was measured at different time points. The sizes of tumor derived from tumor xenografts inoculated with vector alone, on average, produced tumor sizes at day 12 of range 7–11 mm^3 (average 9.4 mm^3), at day 21 of range 6–14 mm^3 (average 9.8 mm^3), at day 25 of range 13–23 mm^3 (average 17 mm^3), and at day 29 of range 32–54 mm^3 (average 36 mm^3). The sizes of tumor derived from tumor xenografts inoculated with HSV-aTIMP-3, on average, produced tumor sizes at day 12 of range 6–13 mm^3 (average 9.8 mm^3), at day 21 of range 5–28 mm^3 (average 10.5 mm^3), at day 25 of range 10–32 mm^3 (average 17.1 mm^3), and at day 29 of range 13–61 mm^3 (average 30.5 mm^3). Tumor sizes derived from tumor xenografts inoculated with HSV-sTIMP-3, on average, produced tumor sizes at day 12 of range 2–5 mm^3 (average 3.4 mm^3), at day 21 of range 2–8 mm^3 (average 4.9 mm^3), at day 25 of range 4–15 mm^3 (average 7.9 mm^3), and at day 29 of range 5–10 mm^3 (average 7.9 mm^3).

nificant numbers of DNA 3'-OH ends were not stained red. Our results are therefore consistent with the notion that the apoptotic responses induced by TIMP-3 involve the activation of caspases, proteolysis of downstream targets for caspases, as well as fragmentation of nucleosomal DNA.

Similar to an earlier report suggesting the induction of a cytotoxic bystander effect that does not require cell-cell contact following the expression of TIMP-3 with adenoviral vectors [39], we observed that some uninfected cells were also positively stained with the TUNEL assay. It is possible that the death of the uninfected cells could be

due to the cytotoxic bystander effect of a low level of soluble TIMP-3 in the microenvironment. Alternatively, altered DNA methylation of the CpG islands of the promoter of the *TIMP3* gene has been reported in human astrocytomas [40–42]; this could lead to a high level of aberrant, but functional, TIMP-3 transcripts that were not detected by our Western blot assays. The methylation status and/or other abnormalities of the *TIMP3* gene in Gli36 cells have yet to be studied. Nevertheless, this finding supports a study in which cell death was observed in melanoma cells incubated in the presence of conditioned medium removed from recombinant adenoviral vector expressing TIMP-3 [39].

TIMP-3 Inhibits Growth of Glioma Xenografts

We also studied the tumor growth-inhibitory effect of TIMP-3 using human tumor xenografts. Since Gli36 cells do not induce tumors in SCID mice consistently, we employed the human U87MG glioma cells for this study. We infected U87MG cells with HSV-sTIMP-3 under experimental conditions similar to those described for Gli36 cells (Fig. 2D). We determined cell viability following infection with HSV-sTIMP-3 over a period of 72 h, as in the case for the Gli36 cells. The observed cell viability for U87MG cells infected with HSV-sTIMP-3 was significantly less than for cells transduced with viruses carrying the viral backbone and the HSV-aTIMP-3 construct at all the time points assayed (Fig. 2D). We could observe no significant differences between the total cell numbers in uninfected cells compared with empty vector-infected cells (data not shown). To study the tumor growth-inhibitory effect of TIMP-3, we administered 1×10^6 transduction units of the HSV-sTIMP-3 amplicon viral vectors into the flank region of SCID CB17 immunodeficient mice that had been inoculated with U87MG cells 24 h earlier. Compared to mice that were infected with viruses carrying the viral backbone and the HSV-aTIMP-3 construct, the kinetics of tumor development in U87MG-bearing mice infected with viruses carrying the HSV-sTIMP-3 amplicon viral construct was much reduced (Fig. 2E). The measurable sizes of tumors in mice of the HSV-sTIMP-3-infected group were significantly smaller than those of mice infected with the backbone empty viral vectors ($P < 0.01$) and those infected with the HSV-aTIMP-3 construct ($P < 0.01$) (Fig. 2E). In comparison, the measurable sizes of tumors were not significantly different between U87MG-bearing mice infected with the HSV-aTIMP-3 viral construct and mice infected with viruses carrying the backbone amplicon vector ($P > 0.05$) (Fig. 2E). We performed the experiment independently twice, with comparable results. Further, there was no significant inhibition of tumor growth between mice infected with the HSV-sTIMP-3 viruses and the control group beyond day 29 from the time of injection with viruses (data not shown). This may perhaps suggest that the observed cytotoxic effect of TIMP-3 is not sufficient to eradicate all

the rapidly proliferating tumor cells due to the low percentage of tumor cells that were originally infected with the HSV-sTIMP-3 viruses.

In the present study, all human glioma cells gave high levels of TIMP-3 protein expression by Western blot analysis (Fig. 1A) and underwent cell death as determined by TUNEL assay (Fig. 2C) following infection with HSV-sTIMP-3. In addition to demonstrating the possibility of employing TIMP-3 as an effective adjuvant therapy to target residual brain tumor cells, the present study provides a molecular insight into the effects of TIMP-3 on survival factors/death effectors. It is apparent that the ability of TIMP-3 to prevent shedding of death receptors and inhibit angiogenesis could only partly explain the retardation of progression of glioma xenografts. The overexpression of TIMP-3 has been demonstrated molecularly to be associated with wide ranges of substrates of the MMP family and, thus, it would be dependent on the ability to balance the interactions of these cell growth/death signal molecules within the tumor microenvironment to exploit fully the pharmacological potentials of TIMP-3.

MATERIALS AND METHODS

Cell culture. The human glioma cell line U87MG was obtained from The American Type Culture Collection (Manassas, VA, USA). The human glioma cell lines SF767 and U251 were kind gifts from D. F. Deen (Brain Tumor Research Center, UCSF, School of Medicine, San Francisco, CA, USA), while the glioma cell line Gli36 was kindly provided by A. T. Campagnoni (UCLA School of Medicine, Los Angeles, CA, USA). Cell line 7374-3D6 was derived from an AAV-latently infected epithelial lung carcinoma (gift from R. Kotin, NIH, Bethesda, MD, USA). African green monkey kidney 2-2 cells, which are Vero-derived cells and constitutively express the HSV-1 ICP27 proteins (kindly provided by R. Sandri-Goldin, UCLA) [21], were cultivated in the presence of Geneticin (500 μ g/ml; Invitrogen Life Technologies, Grand Island, NY, USA). All cells were grown as monolayers in Dulbecco's modified Eagle medium supplemented with 10% fetal bovine serum (HyClone Laboratories, Logan, UT, USA), penicillin (100 U/ml; Invitrogen Life Technologies), streptomycin (100 μ g/ml; Invitrogen Life Technologies), and 2 mM L-glutamine (Sigma-Aldrich, St. Louis, MO, USA) at 37°C in a 5% CO₂-95% air atmosphere.

RT-PCR. Human TIMP-3 cDNA fragment was reverse transcribed and amplified from total RNA prepared from the cell line 7374-3D6 according to the instructions provided with Trizol reagents (Invitrogen Life Technologies). The PCR primers used were as follows: TIMP-3F281, 5'-TTTGGATCCAGCGGCAATGACCCCTTGG; TIMP-3RXHOI, 5'-AAACTC-GAGCAGGGTCTGGCGCTCAGGG.

Second-strand cDNA synthesis was performed with Superscript II RNase H reverse transcriptase (Invitrogen Life Technologies). Each RT-PCR was performed in a final volume of 50 μ l, with 1.5 μ l of RT products as the template. The PCR amplification was performed under the following conditions: 95°C for 5 min (first cycle only); 95°C for 30 s, 50°C for 1 min, 72°C for 1 min (29 cycles); followed by a final extension of 72°C for 10 min. The PCR product was gel purified (Bio 101 GeneClean Kit, La Jolla, CA, USA) and cloned into the backbone amplicon plasmid vector pHGCX (kindly provided by Y. Saeki, Massachusetts General Hospital, Boston, MA, USA) and verified by DNA sequencing (Applied Biosystems, Foster City, CA, USA).

Helper virus-free packaging. Packaging of HSV-1 amplicons into the HSV-1 virions has been described previously [22]. Briefly, 2-2 cells (3×10^6

cells) were cotransfected with 1.0 μg of amplicon DNA and bacterial artificial chromosome fHSV $\Delta\text{pac}27$ 0+ [23] using the LipofectAmine procedure (Invitrogen Technologies). Sixty hours posttransfection, the cells were scraped into medium; the suspension was frozen and thawed three times and sonicated for 17 s at setting 3.5 (550 Sonic Dismembrator; Fisher Scientific, Hampton, NH, USA) and cellular debris was removed by centrifugation for 10 min at 2000g. The filtrate was then concentrated and purified by centrifugation through a 25% sucrose gradient and centrifuged in a Beckman Coulter (Fullerton, CA, USA) SW28 rotor at 25,000 rpm for 4 h at 4°C. The resulting pellet was resuspended overnight in Hanks' balanced salt solution (Invitrogen Life Technologies) and stored in 100- μl aliquots at -80°C. To determine vector titers (TU/ml), 2-2 cells were infected and, 24 h later, green fluorescent cells were counted under a fluorescence microscope.

In vitro transduction and induction of cell culture cytotoxicity. To determine the *in vitro* cytopathic efficacy of HSV-sTIMP-3, 1.5×10^5 human glioma cells were seeded in each well of a six-well plate (Nunc, Roskilde, Denmark) 24 h prior to infection. On the following day, cells were infected with the empty, HSV-sTIMP-3, or HSV-aTIMP-3 amplicon viral vector at m.o.i. of 1.0. At the required time points, viable adherent cells from triplicate cultures were determined using the trypan blue exclusion assay.

Western blot analysis. Briefly, 5×10^5 Gli36 cells seeded in a 100-mm tissue culture dish were infected with empty vector, HSV-sTIMP-3, or HSV-aTIMP-3 at m.o.i. of 1.0 and incubated for 72 h. Cells were washed twice with PBS and harvested with a cell scraper. Lysis buffer (50 mM Tris, 150 mM NaCl, 1% Triton X-100) was added to the cell pellet in the presence of protease inhibitor cocktail (Roche Diagnostic, Mannheim, Germany) for 30 min on ice. The cell lysate was centrifuged at 4°C for 15 min at 15,000g. Protein lysates (100 μg) were separated by SDS-PAGE and immunoblotted with either polyclonal antibody against TIMP-3 (1:300 dilution, Chemicon) or control anti- β -tubulin mouse IgM (1:500 dilution; BD Biosciences Pharmingen, San Diego, CA, USA) for 1 h. The membrane was then incubated with secondary anti-rabbit (1:500 dilution) or mouse (1:1000 dilution) horseradish peroxidase-conjugated antibodies (Dako-Cytomation, Glostrup, Denmark) for 30 min at room temperature and subjected to ECL reaction (Santa Cruz Biotechnology, Santa Cruz, CA, USA).

TUNEL analysis. Human glioma Gli36 cells (4×10^4 cells) were infected with HSV-sTIMP-3 at an m.o.i. of 1.0. Transduced cells at 72 h p.i. were fixed with 1% paraformaldehyde for 20 min, and TUNEL assay was performed following the instructions of the ApopTag apoptosis detection kit manual (Intergen, Purchase, NY, USA). Briefly, the fixed cells were incubated with TdT enzyme in the presence of digoxigenin-labeled dNTP, followed by rhodamine-conjugated anti-digoxigenin antibody. Cells were then mounted using Vectashield mounting medium containing DAPI (1 $\mu\text{g}/\text{ml}$; Vector Laboratories, Burlingame, CA, USA) and examined using an LSM 510 confocal microscope (Carl Zeiss Microscopy, Göttingen, Germany) with appropriate filters.

Animal studies. Three groups ($n = 5$) of 6- to 8-week-old CB-17 SCID mice (Animal Resource Centre, Canning Vale, Western Australia, Australia) were subcutaneously injected with human glioma U87MG cells (1×10^6). A total of 1×10^6 transduction units of HSV-sTIMP-3, HSV-aTIMP-3, or control amplicon viral vector was administered into the marked tumor site where tumor cells were implanted 24 h earlier. The tumor growth was subsequently monitored at different time points and its volume was calculated using the formula tumor volume (mm^3) = $0.52 \times \text{width (mm)}^2 \times \text{length (mm)}$ [24].

Statistical analysis. Data are presented throughout this study as means \pm standard error of the mean. Statistical significance was determined by paired *t* test in the *in vitro* study and ANOVA in the *in vivo* study, where $P < 0.05$ was considered significant.

Array hybridization and staining. Total RNA was extracted from both Gli36 cells and cells infected with HSV-sTIMP-3 using an infection condition similar to Western blot analysis described above. Isolation of

total RNA using TRIzol reagent (Invitrogen) has also been described earlier [25]. Amplified RNA (15 μg) was used to hybridize to HG-133A gene chip array (Affymetrix) according to the manufacturer's protocol. Three independent experiments were performed with each experiment consisting of both uninfected control cells and HSV-sTIMP-3-infected cells.

Data analysis. Data analysis and absent/present call determination were performed on raw fluorescence intensity values using Affymetrix Data Mining Tool 3.0 software. "Present" calls were calculated by estimating whether a transcript was detected in a sample based on the strength of the signal of the gene compared with background. Only genes with present calls either in all infected or in all control samples were analyzed. The data generated in chp file format was later exported and filtered with cutoff value of 0.26 signal-log ratio (or the equivalence of 1.2 in terms of fold change) using Affymetrix Data Mining Tool 3.0 software to generate a list of genes with differential expression. The selected genes were then annotated using the Affymetrix NetAffx GeneOntology analysis system (<http://www.affymetrix.com>). All infected and control samples were normalized against 100 maintenance genes prior to performing comparison analysis. This was to minimize discrepancies among arrays due to variables such as sample preparation, hybridization, staining, or probe array lot. Statistical analysis between the infected and the control groups was performed using unpaired *t* test ($P < 0.05$).

ELISA. Caspase-1 (R&D Systems, Minneapolis, MN, USA) and TNF- α (Chemicon) were measured according to the manufacturer's instructions using commercial ELISA kits. The amplicon viral infection and cell lysate preparation were previously described under Western blot analysis. All samples were assayed in triplicate.

ACKNOWLEDGMENTS

We express our thanks to Dr. Tan Hiang Khoon (Singapore General Hospital, Singapore) and Mr. Yuan Chu-Jun (University of Rochester, Rochester, NY, USA) for their valuable discussions and support concerning this study. This research was supported by grants from the Agency for Science, Technology and Research (A*STAR), Singapore, and the Singapore National Medical Research Council, Singapore.

RECEIVED FOR PUBLICATION JUNE 15, 2004; ACCEPTED FEBRUARY 7, 2005.

APPENDIX A. SUPPLEMENTARY DATA

Supplementary data associated with this article can be found, in the online version, at doi:10.1016/j.jymthe.2005.02.028

REFERENCES

- Stetler-Stevenson, W. G., Liotta, L. A., and Kleiner, D. E., Jr. (1993). Extracellular matrix. 6. Role of matrix metalloproteinases in tumor invasion and metastasis. *FASEB J.* **7**: 1434–1441.
- Birkedal-Hansen, H., et al. (1993). Matrix metalloproteinases: a review. *Crit. Rev. Oral Biol. Med.* **4**: 197–250.
- Nagase, H. (1997). Activation mechanisms of matrix metalloproteinases. *Biol. Chem.* **378**: 151–160.
- Brinckerhoff, C. E., and Matrisian, L. M. (2003). Matrix metalloproteinases: a tail of a frog that became a prince. *Nat. Rev. Mol. Cell. Biol.* **3**: 207–214.
- Hernandez-Barrantes, S., et al. (2002). Regulation of membrane type-matrix metalloproteinases. *Semin. Cancer Biol.* **12**: 131–138.
- Chintala, S. K., Tonn, J. C., and Rao, J. S. (1999). Matrix metalloproteinases and their biological function in human gliomas. *Int. J. Dev. Neurosci.* **5–6**: 495–502.
- Jiang, Y., Goldberg, I. D., and Shi, Y. E. (2002). Complex roles of tissue inhibitors of metalloproteinases in cancer. *Oncogene* **21**: 2245–2252.
- Hojilla, C. V., Mohammed, F. F., and Khokha, R. (2003). Matrix metalloproteinases and their tissue inhibitors direct cell fate during cancer development. *Br. J. Cancer* **89**: 1817–1821.
- Gomez, D. E., Alonso, D. F., Yoshiji, H., and Thorgeirsson, U. P. (1997). Tissue inhibitors of metalloproteinases: structure, regulation and biological functions. *Eur. J. Cell Biol.* **74**: 111–122.
- Brew, K., Dinakarpanian, D., and Nagase, H. (2000). Tissue inhibitors of metalloproteinases: evolution, structure and function. *Biochim. Biophys. Acta* **1477**: 267–283.

11. Baker, A. H., Edwards, D., and Murphy, G. (2002). Metalloproteinase inhibitors: biological actions and therapeutic opportunities. *J. Cell Sci.* **115**: 3719–3727.
12. Amour, A., et al. (1998). TNF-alpha converting enzyme (TACE) is inhibited by TIMP-3. *FEBS Lett.* **435**: 39–44.
13. Li, G., Fridman, R., and Kim, H. R. (1999). Tissue inhibitor of metalloproteinase-1 inhibits apoptosis of human breast epithelial cells. *Cancer Res.* **59**: 6267–6275.
14. Valente, P., et al. (1998). TIMP-2 over-expression reduces invasion and angiogenesis and protects B16F10 melanoma cells from apoptosis. *Int. J. Cancer* **75**: 246–253.
15. Jiang, Y., et al. (2001). Stimulation of mammary tumorigenesis by systemic tissue inhibitor of matrix metalloproteinase 4 gene delivery. *Cancer Res.* **61**: 2365–2370.
16. Anand-Apte, B., et al. (1996). A review of tissue inhibitor of metalloproteinases-3 (TIMP-3) and experimental analysis of its effect on primary tumor growth. *Biochem. Cell Biol.* **74**: 853–862.
17. Smith, M. R., Kung, H., Durum, S. K., Colburn, N. H., and Sun, Y. (1997). TIMP-3 induces cell death by stabilizing TNF-alpha receptors on the surface of human colon carcinoma cells. *Cytokine* **9**: 770–780.
18. Hargreaves, P. G., et al. (1998). Human myeloma cells shed the interleukin-6 receptor: inhibition by tissue inhibitor of metalloproteinase-3 and a hydroxamate-based metalloproteinase inhibitor. *Br. J. Haematol.* **101**: 694–702.
19. Ahonen, M., et al. (2003). Tissue inhibitor of metalloproteinases-3 induces apoptosis in melanoma cells by stabilization of death receptors. *Oncogene* **22**: 2121–2134.
20. Bond, M., Murphy, G., Bennett, M. R., Newby, A. C., and Baker, A. H. (2002). Tissue inhibitor of metalloproteinase-3 induces a Fas-associated death domain-dependent type II apoptotic pathway. *J. Biol. Chem.* **277**: 13787–13795.
21. Smith, I. L., Hardwicke, M. A., and Sandri-Goldin, R. M. (1992). Evidence that the herpes simplex virus immediate protein ICP27 acts post-transcriptionally during infection to regulate gene expression. *Virology* **186**: 74–86.
22. Ho, I. A. W., Hui, K. M., and Lam, P. Y. P. (2004). Glioma-specific and cell cycle regulated HSV-1 amplicon viral vector. *Hum. Gene Ther.* **15**: 495–508.
23. Saeki, Y., Breakefield, X. O., and Chiocca, E. A. (2003). Improved HSV-1 amplicon packaging system using ICP27-deleted, oversized HSV-1 BAC DNA. *Methods Mol. Med.* **76**: 51–60.
24. Bergers, G., Javaherian, K., and Lo, K. M. (1999). Effects of angiogenesis inhibitors on multistage carcinogenesis in mice. *Science* **284**: 808–812.
25. Tan, M. G., et al. (2004). Cloning and identification of hepatocellular carcinoma down regulated mitochondrial carrier protein, a novel liver-specific uncoupling protein. *J. Biol. Chem.* **279**: 45235–45244.
26. Amour, A., et al. (2000). The in vitro activity of ADAM-10 is inhibited by TIMP-1 and TIMP-3. *FEBS Lett.* **473**: 275–279.
27. Loechel, F., Fox, J. W., Murphy, G., Albrechtsen, R., and Wewer, U. M. (2000). ADAM 12-5 cleaves IGFBP-3 and IGFBP-5 and is inhibited by TIMP-3. *Biochem. Biophys. Res. Commun.* **278**: 511–515.
28. Kashiwagi, M., Tortorella, M., Nagase, H., and Brew, K. (2001). TIMP-3 is a potent inhibitor of aggrecanase 1 (ADAM-TS4) and aggrecanase 2 (ADAM-TS5). *J. Biol. Chem.* **276**: 12501–12504.
29. Kuno, K., Terashima, Y., and Matsushima, K. (1999). ADAMTS-1 is an active metalloproteinase associated with the extracellular matrix. *J. Biol. Chem.* **274**: 18821–18826.
30. Black, R. A., et al. (1997). A metalloproteinase disintegrin that releases tumour-necrosis factor-alpha from cells. *Nature* **385**: 729–733.
31. Peschon, J. J., et al. (1998). An essential role for ectodomain shedding in mammalian development. *Science* **282**: 1281–1284.
32. Klenotic, P. A., et al. (2004). Tissue inhibitor of metalloproteinases-3 (TIMP-3) is a binding partner of epithelial growth factor-containing fibulin-like extracellular matrix protein 1 (EFEMP1): implications for macular degenerations. *J. Biol. Chem.* **279**: 30469–30473.
33. Timpl, R., et al. (2003). Fibulins: a versatile family of extracellular matrix proteins. *Nat. Rev. Mol. Cell Biol.* **4**: 479–489.
34. Werb, Z. (1997). ECM and cell surface proteolysis: regulating cellular ecology. *Cell* **91**: 439–442.
35. Qi, J. H., et al. (2003). A novel function for tissue inhibitor of metalloproteinases-3 (TIMP3): inhibition of angiogenesis by blockage of VEGF binding to VEGF receptor-2. *Nat. Med.* **9**: 407–415.
36. Sallinen, S. L., et al. (2000). Identification of differentially expressed genes in human gliomas by DNA microarray and tissue chip techniques. *Cancer Res.* **60**: 6617–6622.
37. Beissbarth, T., and Speed, T. P. (2004). GOstat: find statistically overrepresented gene ontologies within a group of genes. *Bioinformatics* **20**: 1464–1465.
38. Degterev, A., Boyce, M., and Yuan, J. (2003). A decade of caspases. *Oncogene* **22**: 8543–8567.
39. Ahonen, M., et al. (2002). Antitumor activity and bystander effect of adenovirally delivered tissue inhibitor of metalloproteinases-3. *Mol. Ther.* **5**: 705–715.
40. Gonzalez-Gomez, P., et al. (2004). Promoter methylation status of multiple genes in brain metastases of solid tumors. *Int. J. Mol. Med.* **13**: 93–98.
41. Gonzalez-Gomez, P., et al. (2003). Promoter hypermethylation of multiple genes in astrocytic gliomas. *Int. J. Oncol.* **22**: 601–608.
42. Bachman, K. E., et al. (1999). Methylation associated silencing of the tissue inhibitor of metalloproteinase 3 gene suggests a suppressor role in kidney, brain, and other human cancers. *Cancer Res.* **59**: 798–802.